

Small Particle Driven Chain Disentanglements in Polymer Nanocomposites

Erkan Senses,^{1,2,*} Siyam M. Ansar,³ Christopher L. Kitchens,³ Yimin Mao,^{1,2} Suresh Narayanan,⁴ Bharath Natarajan,⁵ and Antonio Faraone^{1,†}

¹*NIST Center for Neutron Research, National Institute of Standards and Technology, Gaithersburg, Maryland 20899-8562, USA*

²*Department of Materials Science and Engineering, University of Maryland, College Park, Maryland 20742-2115, USA*

³*Department of Chemical and Biomolecular Engineering, Clemson University, Clemson, South Carolina 29634, USA*

⁴*Advanced Photon Source, Argonne National Laboratory, Argonne, Illinois 60439, USA*

⁵*Materials Measurement Laboratory, National Institute of Standards and Technology, Gaithersburg, Maryland 20899, USA*

(Received 29 November 2016; revised manuscript received 27 January 2017; published 5 April 2017)

Using neutron spin-echo spectroscopy, x-ray photon correlation spectroscopy, and bulk rheology, we studied the effect of particle size on the single-chain dynamics, particle mobility, and bulk viscosity in athermal polyethylene oxide-gold nanoparticle composites. The results reveal a $\approx 25\%$ increase in the reptation tube diameter with the addition of nanoparticles smaller than the entanglement mesh size (≈ 5 nm), at a volume fraction of 20%. The tube diameter remains unchanged in the composite with larger (20 nm) nanoparticles at the same loading. In both cases, the Rouse dynamics is insensitive to particle size. These results provide a direct experimental observation of particle-size-driven disentanglements that can cause non-Einstein-like viscosity trends often observed in polymer nanocomposites.

DOI: 10.1103/PhysRevLett.118.147801

The addition of nanoparticles (NPs) into polymeric matrices causes remarkable changes in the physical properties of the composites relative to the host polymer [1]. Particularly interesting and quite unexpected is the non-Einstein-like viscosity reduction often observed in composites with NPs of sizes comparable to that of a single chain [2]. This is contrary to the classical models that always predict an increase in viscosity upon particle addition [3]. As the particle and polymer size become comparable, their motion is expected to be coupled. Understanding how the motion of one component is affected by the presence of the other is important for fundamental science as well as for optimization of nanocomposite properties for advanced materials applications.

The NP relaxation is commonly studied by x-ray photon correlation spectroscopy (XPCS) using tracer nanoparticles in polymeric liquids [4–7]. It is now understood that the motion of NPs smaller than the entanglement mesh size is dictated by local Rouse dynamics of the chains while larger particles are significantly slowed down by the entanglements, resulting in a subdiffusive motion [8,9]. The NP effect on the dynamics of the polymer in the nanocomposites has also been the focus of many experimental and theoretical works, most of which consider large NPs [10–17]. A recent molecular dynamics simulation [17] and primitive path analysis [16] emphasizes the particle-size effects on the local segmental dynamics in attractive and repulsive systems. Very rich dynamical effects, ranging from entanglement dilation to reduced local relaxation, have been predicted for NP sizes comparable to entanglement mesh. Experimentally, how the self and collective chain dynamics are affected by NPs that are as small as the entanglement spacing has not been clarified, mainly due to

the lack of spatial and temporal resolution in conventional experimental techniques.

In this Letter, we apply neutron spin-echo spectroscopy (NSE) on athermal and isotopically labeled poly(ethylene glycol) (PEG) (a low- M_w analog of poly(ethylene oxide) (PEO)) functionalized gold (Au) NP-filled PEO composites to evaluate the role of particle size on the single chain dynamics at a space-time resolution relevant to the segmental and the collective polymer motion in a melt. The results present experimental evidence of a significant tube dilation caused by particles smaller than the entanglement mesh size. No significant effect, however, is observed on the local relaxation. The slow NP motion was probed by XPCS, revealing a compressed and subdiffusive relaxation behavior of small and large NPs, respectively. The effects of decreasing topological confinement on the bulk viscoelastic behavior of the nanocomposites are discussed along with the rheological trends.

The hydrogenated PEO (*h*PEO) ($M_w = 35$ kg/mol, $M_w/M_n = 1.08$) and the deuterated PEO (*d*PEO) ($M_w = 35$ kg/mol, $M_w/M_n = 1.09$) samples, both well above the entanglement molecular weight, $M_e = 2$ kg/mol, were supplied by Polymer Source Inc. and dried further under vacuum at 90 °C for 12 h. The synthesis and characterization of PEG functionalized Au nanoparticles are described elsewhere [18]. The PEG chains on the surface are too short ($M_w = 1$ kg/mol) to entangle; their role is to provide steric repulsion between NPs. The nanocomposites with NPs of diameter 3.5 ± 0.7 nm (PEG grafting density 2.43 molecules/nm²) and 20.2 ± 4.3 nm (PEG grafting density 2.75 molecules/nm²) were prepared by dissolving the particles and PEO separately in acetonitrile (Sigma Aldrich, anhydrous). (The uncertainties

throughout this Letter represent one standard deviation.) The d/h ratio of PEO was 74/26, which matches the scattering from Au nanoparticles. The NPs in acetonitrile were then added to the polymer solutions and cast in Teflon cups to result in a particle volume fraction of 20% ($\phi_{\text{part}} = 0.20$) in the final nanocomposite. The samples were dried overnight and vacuum annealed at 363 K for 2 days to ensure removal of any residual solvent (see Supplemental Material for composite structures [19]). The particle-free d/h PEO was prepared using an identical casting and annealing protocol. Additional dilute nanocomposite samples in h PEO (particles weight fraction of 1%) were prepared for XPCS measurements.

Small-angle neutron scattering (SANS) experiments were performed on beam line NG-7 at the NIST Center for Neutron Research (NCNR, Gaithersburg, MD). The Q range covered was from $\approx 0.003 \text{ \AA}^{-1}$ to 0.5 \AA^{-1} . All scattering profiles were corrected for background, empty cell, and sample transmission to get 1D isotropic scattering patterns. Collective PEO dynamics were obtained using the NGA Neutron Spin Echo Spectrometer at the NIST Center for Neutron Research (NCNR, Gaithersburg, MD). The measurements were performed at 400 K using a wavelength of $\lambda = 11 \text{ \AA}$ ($\Delta\lambda/\lambda = 0.15$) for Fourier times up to 100 ns and a wave vector range of $Q = 0.08 \text{ \AA}^{-1}$ to 0.2 \AA^{-1} . Additional measurements were performed at $\lambda = 6 \text{ \AA}$ for Fourier times up to 15 ns. The samples were sealed in Al cans in a helium environment. Charcoal was used to obtain the instrumental resolution. Data were corrected for background using an empty can measurement using the software dave [22]. Rheology experiments were performed on a strain-controlled ARES-G2 (TA instruments) rheometer equipped with 25-mm parallel plate fixtures. XPCS measurements were performed using a photon energy of 11 keV on beamline 8-ID-I at the Advanced Photon Source at Argonne National Laboratory. Samples were equilibrated at 400 K for 15 min prior to measurements. The normalized intensity-intensity autocorrelation function, $g_2(Q, t)$, was obtained over the wave vector range $0.003 \text{ \AA}^{-1} < Q < 0.02 \text{ \AA}^{-1}$ and analyzed at 36 discrete Q values.

The inset of Fig. 1 shows the SANS profiles for the neat polymer and the composites with 20-nm and 3.5-nm NPs that are zero-average-contrast matched to the matrix. All profiles converge to give the scaling $I(Q) \sim Q^{-2}$ at $Q > 0.04 \text{ \AA}^{-1}$ due to the single-chain form factor of PEO in the mixture of d PEO and h PEO. Fitting the neat polymer profile for $Q > 0.008 \text{ \AA}^{-1}$ to the Debye form factor yields the coil size, $R_g \approx 7.5 \text{ nm}$, a value close to the predicted number [23]. The Kratky plots obtained after subtracting the incoherent background, $Q^2 I(Q)$ vs Q [19], show a well-defined plateau in this regime, suggesting that the Gaussian statistics of PEO is retained in both composite samples. The peak at $Q \approx 0.035 \text{ \AA}^{-1}$ in the 20-nm NP composite corresponds to a length scale $D \approx 18 \text{ nm}$, a number close to the

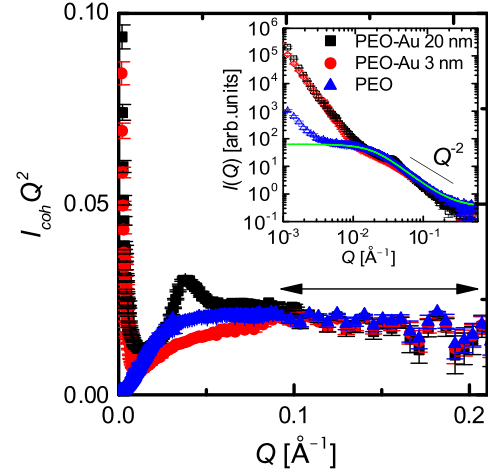


FIG. 1. Kratky plot of the contrast matched composites, $\phi_{\text{part}} = 0.20$, and h/d (74/26) PEO matrices. The arrow represents the spatial range used in NSE. The inset shows the SANS profiles and the Debye fitting to the neat polymer data.

individual particle size, and can be attributed to the correlation of the PEG chains attached to the particle surface. A similar correlation peak in the nanocomposite with 3.5-nm NPs appears at $Q \approx 0.1 \text{ \AA}^{-1}$; its intensity is negligible compared to the signal from the PEO. The low- Q upturns are identical for nanocomposites with both NP sizes and they are present even in the homopolymer mixture, indicating that this feature is likely related to the excess scattering due to the large-scale composition fluctuations in the matrix and slight scattering-length density mismatch between the polymer and the particles [24]. Regardless, these effects become negligible in the spatial range of NSE, where the scattering is exclusively due to PEO chains.

The effect of particle size on chain dynamics is measured by NSE using a mixture of deuterated and hydrogenated PEO chains. The single chain dynamic structure factor, $S(Q, t)$, is obtained at the spatiotemporal range relevant to a local reptation motion. Figure 2(a) shows the data for $t < 15 \text{ ns}$ corresponding to the initial unrestricted Rouse motions. The profiles are identical; there is no significant effect of particle size on the segmental relaxation rates. This is consistent with previous finding on nanocomposites with neutral polymer-NP interactions [25]. The lines in Fig. 2(a) are the predicted Rouse decays in the absence of entanglements [26]. The dynamics is slowed down as soon as $t \approx 10 \text{ ns}$ due to entanglements; the reptation motion dominates the dynamics in the intermediate time scale. The collective dynamics within the confining tube is well described by de Gennes's model [27] as

$$\frac{S(Q, t)}{S(Q, 0)} = \left[1 - \exp\left(-\frac{Q^2 d^2}{36}\right) \right] S_{\text{local}}(Q, t) + \exp\left(-\frac{Q^2 d^2}{36}\right) S_{\text{esc}}(Q, t) \quad (1)$$

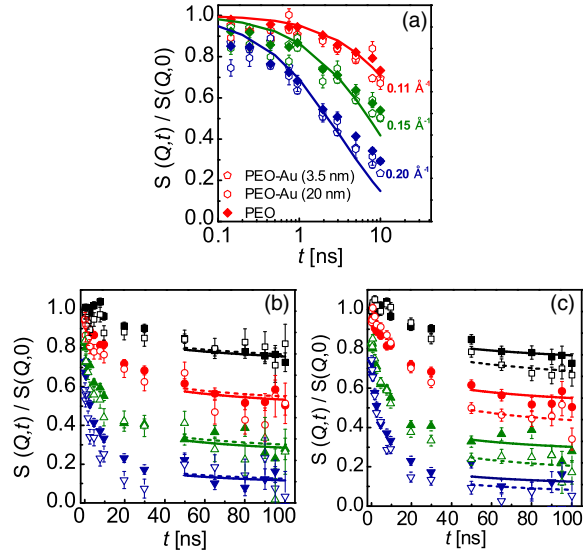


FIG. 2. Dynamic structure factor of the neat PEO (filled symbols) and the PEO nanocomposites with Au nanoparticles (open symbols) at $T = 400$ K showing (a) identical initial Rouse decays at short times, (b) identical long-time plateau for large NP composite, and (c) reptation tube dilation of small NP composite. The symbols in (b) and (c) are for $Q = 0.08 \text{ \AA}^{-1}$ (square), $Q = 0.11 \text{ \AA}^{-1}$ (circle), $Q = 0.15 \text{ \AA}^{-1}$ (triangle), and $Q = 0.20 \text{ \AA}^{-1}$ (inverse triangle). The lines in (a) are the Rouse model predictions [21]; the lines in (b) and (c) are the global fit results from de Gennes's equation [27] with an elementary Rouse rate, $Wl^4 = 1.51 \text{ nm}^4/\text{ns}$.

where $S_{\text{local}}(Q, t) = \exp(t/\tau_o) \text{erfc}(\sqrt{t/\tau_o})$ is the local reptation within the tube with characteristic time scale $\tau_o = 36/(Wl^4Q^4)$. $S_{\text{esc}}(Q, t)$ is the long-time creeping of the chain out of its original tube and $S_{\text{esc}}(Q, t) = 1$ for the motions probed by NSE in this work as $t_{\text{NSE}} \ll \tau_R (\approx 1 \mu\text{s})$. The long-time plateau level is determined by $\exp(-Q^2d^2/36)$. Using $Wl^4 = 1.51 \text{ nm}^4/\text{ns}$ for PEO at 400 K [21], the only free parameter, the reptation tube diameter, d , was obtained from global fitting Eq. (1) to the data. Since Eq. (1) does not account for the initial unrestricted Rouse motion at short times, fitting was applied for $t > 50$ ns [Figs. 2(b) and 2(c)]. The tube size in nanocomposites with large NPs ($d_{\text{PEO-20nmAu}} = 5.17 \pm 0.19 \text{ nm}$) [Fig. 2(b)] is practically identical to that for the particle-free matrix ($d_{\text{PEO}} = 5.03 \pm 0.10 \text{ nm}$). This is in contrast to the increase of the nanocomposite tube diameter with small NPs ($d_{\text{PEO-3nmAu}} = 6.11 \pm 0.13 \text{ nm}$), revealed by the remarkable decrease of the long-time plateau level with respect to the neat PEO [Fig. 2(c)]. To our knowledge, these results provide the first direct experimental evidence of tube dilation in polymer nanocomposites in the small-particle limit.

The NP size driven increase of the reptation tube size leads to a decrease in entanglement density in the composites without significantly changing the local dynamics. The implications of these results on the nanoparticle motion

as well as on the macroscopic properties are very appealing, as the level of entanglements largely determines and may influence the transport properties of NPs in melts.

We measured the slow nanoparticle motion in melts on dilute samples using XPCS. The intensity-intensity autocorrelation function is related to the intermediate scattering function (ISF), $f(Q, t)$, as $g_2(Q, t) \sim 1 + A \cdot [f(Q, t)]^2$, with A and t being the Siegert factor of the instrument and the delay time, respectively. The ISF is fit to the stretched or compressed exponential functions, $f(Q, t) = \exp[-(t/\tau)^\beta]$, with relaxation time τ and stretching exponent β [representative profiles are given in Fig. 3(a), inset]. The NP relaxation in the composites are very different. The large NPs exhibit slightly stretched exponential relaxation with $\beta \approx 0.8$, in agreement with the theoretical predictions for large particles in an entangled polymeric medium [8].

The relaxation of small NPs is hyperdiffusive with compressed exponent $\beta \approx 1.2-1.5$ and $\tau \propto Q^{-1}$ as hypothesized for small particles hopping between the entanglement cages [28]. Given the fact that the segmental chain dynamics remain unchanged in the composites, the difference in relaxation types is primarily due to different topological effects imposed by the chains on different sized particles, i.e., trapping vs caging. The terminal relaxation time of 35 kg/mol PEO at the XPCS temperature (353 K) is $\approx 1 \text{ ms}$ [25], which is smaller than the XPCS time scale ($\approx 10 \text{ ms}$ to $\approx 100 \text{ s}$). Therefore, the center-of-mass motion of PEO dominates the bulk flow of the matrix and might cause a driftlike motion of the large particles, resulting in $\tau \propto Q^{-1}$ dependence. The viscosity experienced by the large particles of diameter a_{NP} estimated from $kT/a_{\text{NP}} = 6\pi a_{\text{NP}}\eta_{\text{XPCS}}v_{\text{XPCS}}$ [29], where $v_{\text{XPCS}} = (\tau Q)^{-1}$ is the particle velocity and η_{XPCS} is the local viscosity of the medium, is found to be $\approx 180 \text{ Pa s}$, which is close to the zero-shear viscosity estimated from the rheology. The motion of small particles confined within the entanglement tubes cannot be explained in the same way by a drift type of motion, as they are too small.

Lastly, the linear viscoelastic moduli at 353 K are compared in Fig. 4. The terminal relaxation time at this

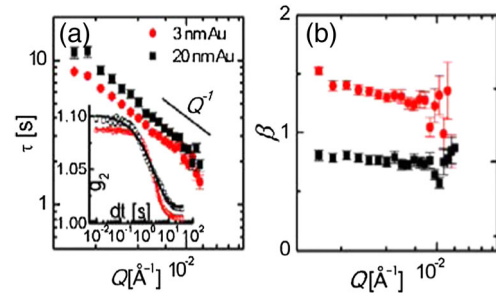


FIG. 3. (a) Relaxation time (τ) and (b) stretching exponent (β) vs Q for PEO composites with a weight fraction of 1% Au nanoparticles. The inset shows a representative autocorrelation function at $Q = 0.01 \text{ \AA}^{-1}$.

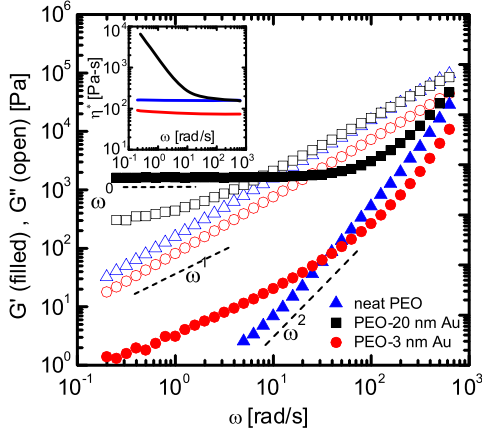


FIG. 4. Linear elastic (G' , filled symbols) and viscous (G'' , open symbols) moduli of the neat matrix and the composites with $\phi_{\text{part}} = 0.20$ NP of different sizes. Complex viscosities, η^* , are plotted in the inset.

temperature ($\tau_d \approx 1$ ms) is well below the time scale of the rheology; the center-of-mass motion of matrix chains directs a liquidlike response with typical Rouse model scaling for elastic and viscous moduli, $G' \propto \omega^2$ and $G'' \propto \omega^1$, respectively. The NPs larger than d result in a strong reinforcement at intermediate and low frequency with $G' \propto \omega^0$, a gel-like response commonly observed for large interacting particles at such high volume fractions [30,31]. The small NP composite at the same volume fraction remains liquidlike with viscosity (≈ 90 Pa s) $\approx 56\%$ of the viscosity of the particle-free matrix (≈ 160 Pa s) (Fig. 4, inset). As $\eta_{\text{bulk}} \propto \tau_d = (3N^3/W\pi^2)(l/d)^2$ and W remains unchanged in the composites, the effect of tube dilation on the bulk viscosity can be estimated as $\eta_{\text{bulk,Au-3nm}}/\eta_{\text{bulk,PEO}} = (d_{\text{PEO}}/d_{\text{PEO-3nmAu}})^2 \approx 0.67 \pm 0.23$; a reasonable agreement is found. Similar dramatic viscosity reductions were observed by Tuteja *et al.* [32,33] on athermal nanocomposites with small polystyrene NPs dispersed in polystyrene matrix. It was hypothesized from indirect measurements that the accelerated motion of NPs in entangled melt and free-volume effects results in reduced viscosities. Our measurements of the single-chain dynamics reveal that the NPs smaller than the entanglement mesh size decrease the number of entanglements per chain. As $d \propto \sqrt{M_{\text{ent}}/M} \propto \sqrt{1/G_N^0}$ where M is the molar mass of the chain, M_{ent} is the molar mass between two entanglement points, and G_N^0 is the equilibrium plateau modulus, we observed $\approx 50\%$ increase in the entanglement molar mass (and expect $\approx 50\%$ decrease of rubbery moduli) in composite with small NPs at $\phi_{\text{part}} \approx 0.2$. It is commonly thought that NPs smaller than d act similar to solvent molecules in athermal polymer melts [17,34]. The analogy, which appears to reasonably estimate the increase in d with $\phi_{\text{Pol}} \approx 0.8$ [since $d(\phi_{\text{Pol}}) = d(\phi_{\text{Pol}} = 1)\phi_{\text{Pol}}^{-0.76}$ [35]], cannot account for the unchanged Rouse dynamics at short times;

the effect of particle size is rather complicated. We also performed NSE experiments (shown in the Supplemental Material [19]) on blends of 1 kg/mol PEG chains (17% volume fraction) in d/h PEO (a composition equivalent to the PEG/PEO ratio in polymer nanocomposite (PNC) with small Au NPs). In such case, the Rouse decay in the blends is significantly faster compared to the neat PEO matrix. This is clearly different than the PNC with small NPs where the short-time decay remained unchanged up to ≈ 30 ns.

In addition to the nanoparticle size, the nanoparticle volume fraction and the polymer-surface interaction play a critical role in determining the chain dynamics. Kalathi *et al.* [17] reported unchanged Rouse dynamics with reduced entanglements in the presence of weakly interacting well-dispersed large particles. They predict slower dynamics at very high particle concentrations when the chains are highly confined, consistent with findings by Glomann *et al.* [14], suggesting a decrease of the apparent tube diameter due to geometric confinement. Composto and co-workers [36] reported reduced center-of-mass diffusion of chains in athermal poly(styrene) (PS)-silica nanocomposites with particles of 13- and 29-nm diameter and attributed this to confinement effect of particles. Note that these particle sizes are above the tube diameter of PS (≈ 8.5 nm) [23]. In their simulation work on a repulsive system, Li *et al.* [16] found that the proposed geometric confinement effect on tube diameter is negligible below the percolation threshold of the spherical particles ($\phi_c \approx 0.31$). Our study considers composites with $\phi_{\text{part}} < \phi_c$, where geometric confinement on entanglement spacing is negligible. In the case of attractive polymer-surface interactions, recent neutron-scattering experiments on composites with large silica nanoparticles and polymers in cylindrical pores suggest decreasing local relaxation rates [25,37]. We conjecture that the competing effects of particle-size-induced disentanglements, chain confinement, and slowing down or unchanged segmental dynamics may result in different macroscopic behavior of attractive nanocomposites.

In summary, the effects of nanoparticle sizes on the single-chain dynamics, nanoparticle mobility, and macroscopic rheology are investigated in athermal polymer nanocomposites using NSE, XPCS, and rheology. The relaxation of large and small NPs is found to exhibit stretched and compressed exponential correlation functions, respectively. The NSE results on the isotopically labeled chains reveal a significant increase of reptation tube size in the presence of small NPs, while no effect is seen for the large NPs. The first direct experimental observation of NP size driven disentanglements together with the unchanged Rouse dynamics have immediate implications on the bulk rheology and help to explain unusual viscosity reduction in polymer nanocomposites.

This work utilized facilities supported in part by the National Science Foundation under Grant No. DMR-1508249 and used resources of the Advanced Photon

Source, a U.S. Department of Energy (DOE) Office of Science User Facility operated for the DOE Office of Science by Argonne National Laboratory under Contract No. DE-AC02-06CH11357. The research was performed in part at the NIST Center for Nanoscale Science and Technology (CNST). Certain trade names and company products are identified in order to specify adequately the experimental procedure. In no case does such identification imply recommendation or endorsement by the National Institute of Standards and Technology, nor does it imply that the products are necessarily the best for the purpose.

*erkan.senses@nist.gov

†antonio.faraone@nist.gov

- [1] R. Krishnamoorti and R. A. Vaia, *Polymer Nanocomposites: Synthesis, Characterization, and Modeling*, ACS Symposium Series Vol. 804 (American Chemical Society Washington, DC, 2002).
- [2] M. E. Mackay, T. T. Dao, A. Tuteja, D. L. Ho, B. Van Horn, H.-C. Kim, and C. J. Hawker, *Nat. Mater.* **2**, 762 (2003).
- [3] G. K. Batchelor, *J. Fluid Mech.* **83**, 97 (1977).
- [4] H. Guo, G. Bourret, M. K. Corbierre, S. Rucareanu, R. B. Lennox, K. Laaziri, L. Piche, M. Sutton, J. L. Harden, and R. L. Leheny, *Phys. Rev. Lett.* **102**, 075702 (2009).
- [5] S. Narayanan, D. R. Lee, A. Hagman, X. Li, and J. Wang, *Phys. Rev. Lett.* **98**, 185506 (2007).
- [6] H. Guo, G. Bourret, R. B. Lennox, M. Sutton, J. L. Harden, and R. L. Leheny, *Phys. Rev. Lett.* **109**, 055901 (2012).
- [7] R. L. Leheny, *Curr. Opin. Colloid Interface Sci.* **17**, 3 (2012).
- [8] L.-H. Cai, S. Panyukov, and M. Rubinstein, *Macromolecules* **44**, 7853 (2011).
- [9] J. T. Kalathi, U. Yamamoto, K. S. Schweizer, G. S. Grest, and S. K. Kumar, *Phys. Rev. Lett.* **112**, 108301 (2014).
- [10] S. Y. Kim, K. S. Schweizer, and C. F. Zukoski, *Phys. Rev. Lett.* **107**, 225504 (2011).
- [11] G. D. Smith, D. Bedrov, and O. Borodin, *Phys. Rev. Lett.* **90**, 226103 (2003).
- [12] P. J. Dionne, R. Ozisik, and C. R. Picu, *Macromolecules* **38**, 9351 (2005).
- [13] T. Glomann, A. Hamm, J. Allgaier, E. G. Hübner, A. Radulescu, B. Farago, and G. J. Schneider, *Soft Matter* **9**, 10559 (2013).
- [14] T. Glomann, G. J. Schneider, J. Allgaier, A. Radulescu, W. Lohstroh, B. Farago, and D. Richter, *Phys. Rev. Lett.* **110**, 178001 (2013).
- [15] G. Schneider, K. Nusser, L. Willner, P. Falus, and D. Richter, *Macromolecules* **44**, 5857 (2011).
- [16] Y. Li, M. Kröger, and W. K. Liu, *Phys. Rev. Lett.* **109**, 118001 (2012).
- [17] J. T. Kalathi, S. K. Kumar, M. Rubinstein, and G. S. Grest, *Soft Matter* **11**, 4123 (2015).
- [18] S. M. Ansar and C. L. Kitchens, *ACS Catal.* **6**, 5553 (2016).
- [19] See Supplemental Material at <http://link.aps.org/supplemental/10.1103/PhysRevLett.118.147801>, which includes Refs. [20, 21], for additional sample characterizations, SANS experimental and analysis details, neutron spin echo results on the blend of short and long chains, and Rouse model parameters.
- [20] R. Poling-Skutvik, K. I. S. Mongcopa, A. Faraone, S. Narayanan, J. C. Conrad, and R. Krishnamoorti, *Macromolecules* **49**, 6568 (2016).
- [21] K. Niedzwiedz, A. Wischnewski, W. Pyckhout-Hintzen, J. Allgaier, D. Richter, and A. Faraone, *Macromolecules* **41**, 4866 (2008).
- [22] R. T. Aзуаh, L. R. Kneller, Y. Qiu, P. L. Tregenna-Piggott, C. M. Brown, J. R. Copley, and R. M. Dimeo, *J. Res. Natl. Inst. Stand. Technol.* **114**, 341 (2009).
- [23] L. Fetters, D. Lohse, and R. Colby, in *Physical Properties of Polymers Handbook* (Springer, New York, 2007), p. 447.
- [24] A.-C. Genix, M. Tatou, A. Imaz, J. Forcada, R. Schweins, I. Grillo, and J. Oberdisse, *Macromolecules* **45**, 1663 (2012).
- [25] E. Senses, A. Faraone, and P. Akcora, *Sci. Rep.* **6**, 29326 (2016).
- [26] D. Richter, M. Monkenbusch, A. Arbe, and J. Colmenero, *Neutron Spin Echo in Polymer Systems* (Springer-Verlag, Berlin, 2005).
- [27] P.-G. de Gennes, *J. Chem. Phys.* **55**, 572 (1971).
- [28] D. Kim, S. Srivastava, S. Narayanan, and L. A. Archer, *Soft Matter* **8**, 10813 (2012).
- [29] R. Mangal, S. Srivastava, S. Narayanan, and L. A. Archer, *Langmuir* **32**, 596 (2016).
- [30] Q. Zhang and L. A. Archer, *Langmuir* **18**, 10435 (2002).
- [31] E. Senses, A. Isherwood, and P. Akcora, *ACS Appl. Mater. Interfaces* **7**, 14682 (2015).
- [32] A. Tuteja, M. E. Mackay, C. J. Hawker, and B. Van Horn, *Macromolecules* **38**, 8000 (2005).
- [33] A. Tuteja, M. E. Mackay, S. Narayanan, S. Asokan, and M. S. Wong, *Nano Lett.* **7**, 1276 (2007).
- [34] J. T. Kalathi, G. S. Grest, and S. K. Kumar, *Phys. Rev. Lett.* **109**, 198301 (2012).
- [35] P.-G. de Gennes, *Scaling Concepts in Polymer Physics* (Cornell University Press, Ithaca, NY, 1979).
- [36] S. Gam, J. S. Meth, S. G. Zane, C. Chi, B. A. Wood, K. I. Winey, N. Clarke, and R. J. Composto, *Soft Matter* **8**, 6512 (2012).
- [37] M. Krutyeva, A. Wischnewski, M. Monkenbusch, L. Willner, J. Maiz, C. Mijangos, A. Arbe, J. Colmenero, A. Radulescu, O. Holderer, M. Ohl, and D. Richter, *Phys. Rev. Lett.* **110**, 108303 (2013).